

Observations of Secondary Flow Induced by a Wharf

Peter Russell¹ and Ross Vennell¹

¹Department of Marine Science, University of Otago, New Zealand

Abstract

Secondary flow is an important mechanism in the transport and accumulation of sediment in curved flows. Curved flows occur in many places, such as in channel bends, at headlands and as shown in this paper around protruding wharfs within ports. Any near bottom flow that is normal to the depth average flow has the potential to transport sediment cross channel. High resolution moving vessel ADCP measurements were made of the Ferguson – Wynyard Wharf area in the Ports of Auckland. Four surveys were conducted over a 13 hour period on different days producing a time series of velocity profiles with a 1 hour sampling rate. Observations of the measurements indicate helical secondary flow in a plane normal to the depth average velocity in areas where there is induced curvature in the flow. This is evident as the flow passes round the tip of the Ferguson wharf, and the area downstream towards the Jellicoe wharf. Observed near bottom velocities of up to 9.0 cms^{-1} radially inward could transport sediment across the flow towards the berthing area.

1 Introduction

Secondary flow is a factor for consideration in the planning of wharf construction and maintenance dredging. The curved flow of tidal currents around a protruding wharf have the potential to induce secondary flow normal to the depth average flow. Near bottom secondary flow is a possible mechanism contributing to sediment transport towards the wharf area. It is not the intention of this paper to explore the dynamics of sediment transport, dispersion and accretion, but to qualitatively describe an example of secondary flow induced by a protruding wharf.

Secondary flow is defined to be flow in the plane normal to the direction of the depth average current and is radially outwards near the surface and radially inwards near the bottom. The magnitude of secondary flow can be up to 10% of the depth average current. Curvature induced secondary flow (Kalkwijk and Booij, 1986) occurs in river bends (Bathurst and Hey, 1977), around headlands (Garrett and Loucks, 1976) and in the case of this paper around a protruding wharf. Secondary flow also occurs within separation eddies generated by headlands (Pingree, 1978). Field measurements have been made of the three dimensional tidal flow around headlands (Geyer, 1993), and in a curved tidal channel (Vennell and Old, 2006).

Secondary flow can be described by using a curvilinear coordinate system, with the stream-wise coordinate, s , orientated in the direction of the depth averaged flow, and the cross-stream coordinate n , orientated normal to this. In terms of velocity the stream-wise component is denoted by u_s , and the cross-stream component by u_n , which is the secondary flow. A model for secondary flow (Kalkwijk and Booij, 1986), is developed by assuming that $u_s \gg u_n$, and the density is uniform with negligible vertical advection. An approximation of the cross-stream momentum equation is then

$$\frac{\partial u_n}{\partial t} + u_s \frac{\partial u_n}{\partial s} - \frac{u_s^2}{R_s} - f u_s^2 + g \frac{\partial \eta}{\partial n} - \frac{\partial}{\partial z} \left(A \frac{\partial u_n}{\partial z} \right) = 0 \quad (1)$$

Where R_s is the radius of curvature, f the Coriolis acceleration, η the water level, and A the eddy viscosity. Taking the depth average form of (1)

$$\overline{u_s \frac{\partial u_n}{\partial s}} - \frac{\overline{u_s^2}}{R_s} + f \overline{u_s} + g \frac{\partial \eta}{\partial n} + \frac{\tau_n}{\rho h} = 0 \quad (2)$$

where τ_n is the bottom friction in the cross-stream direction given by

$$\frac{\tau_n}{\rho} = \left[A \frac{\partial u_n}{\partial z} \right]_{z=-h} \quad (3)$$

By ignoring the depth average stream-wise advection term in (2) as being negligible (Kalkwijk and Booij, 1986), and subtracting the depth average form (2) from the approximated transverse momentum equation (1), the water level term can be eliminated giving an expression for secondary circulation.

$$\frac{\partial u_n}{\partial t} + u_s \frac{\partial u_n}{\partial s} - \frac{\partial}{\partial z} \left(A \frac{\partial u_n}{\partial z} \right) - \frac{\tau_n}{\rho h} = - \frac{u_s^2 - \overline{u_s^2}}{R_s} - f(u_s^2 - \overline{u_s^2}) \quad (4)$$

The right hand side of (4) indicates two forces inducing secondary flow. The first term being the centripetal acceleration due to the stream-wise velocity and the degree of curvature, the second being the Coriolis acceleration due to the Earth's rotation.

This paper focuses on curvature induced secondary flow. The driving forces behind curvature induced secondary flow are a stream-wise velocity shear due to bottom friction and centripetal acceleration. The velocity shear decreases the velocity towards the bottom resulting in an imbalance in the centripetal acceleration. This drives the flow radially outwards near the surface, and radially inwards near the bottom, creating a helical flow pattern around the curve.

2 Method

2.1 ADCP Measurements

Acoustic Doppler Current Profilers (ADCPs) mounted on moving vessels are increasingly being used to

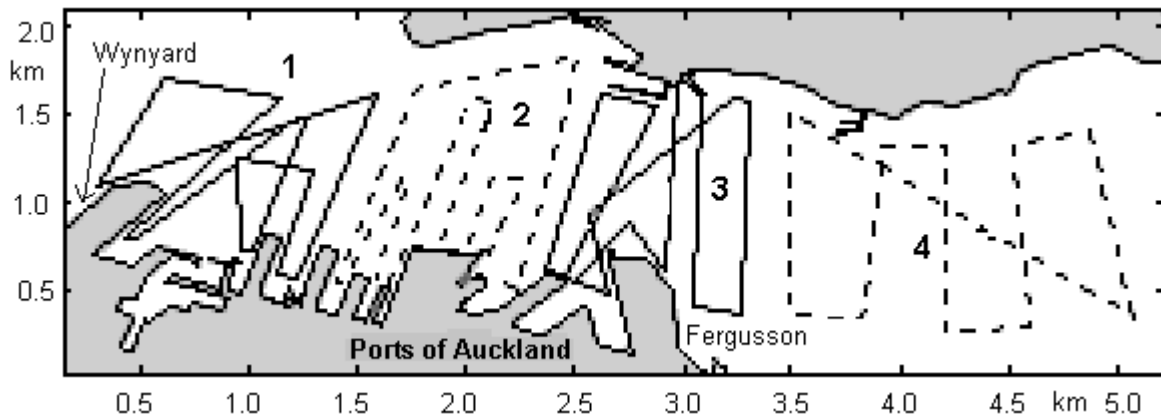


Figure 1 Vessel circuits of four tidal long ADCP measurement surveys of the port of Auckland (R. Vennell).

measure tidal currents in coastal locations including man made areas such as ports. The ADCP is a type of Sonar that uses the Doppler shift from the echo off objects such as plankton and sediment suspended in the water to measure the velocity of the current. These measurements are 3-dimensional, with echos from shallow water being received by the ADCP before echos from deeper water.

The ADCP measurements in this paper are made using a RDI RioGrand 600 KHz ADCP from the 8.5 m survey vessel Astrolabe by the Ports of Auckland hydrographic surveyors. The area surveyed is in the vicinity of the Fergusson – Wynyard wharf area (Figure 1), where by the vessel steamed repeatedly around hour long circuits for a full tidal cycle, 13 hours. These measurements are part of a larger survey of four circuits conducted on both the spring and neap tides. The data from the spring tides are used for this paper. The ADCP recorded velocities in 0.75 m depth bins, averaging 8 pings to give velocity profiles 3.3 seconds apart. With a vessel speed of 4 knots, the raw profiles were about 7m apart. The water depth for most of the circuits was greater than 10 m.

2.2 Tidal Analysis

The velocity structure for the raw data is extracted and any velocities greater than 1.5 ms^{-1} are discarded. During the extraction the raw velocities are rotated so that the stream-wise component, u_s , is aligned with the direction of the depth average velocity \bar{u}_s , (Vennell and Old, 2006). The cross-stream component or secondary flow, u_n , is normal to this. Thus if a rotated raw velocity has zero cross-stream component at a particular depth, it is orientated in the direction of the depth average velocity. Non-zero cross-stream components will be either inward or outward relative to the curvature.

Plots of the raw velocity for each circuit are observed in order to identify areas of interest. Once an area is identified, the raw velocity is plotted at different depths (Figure 2), to look for evidence of secondary flow. The rotated velocities at each depth are averaged though the area to give a depth dependent velocity profile. With each individual depth profile the magnitude of both the stream-wise and cross-stream

component is divided by the magnitude of the depth average velocity, to give a profile of the primary and secondary flow normalised to the depth average respectively.

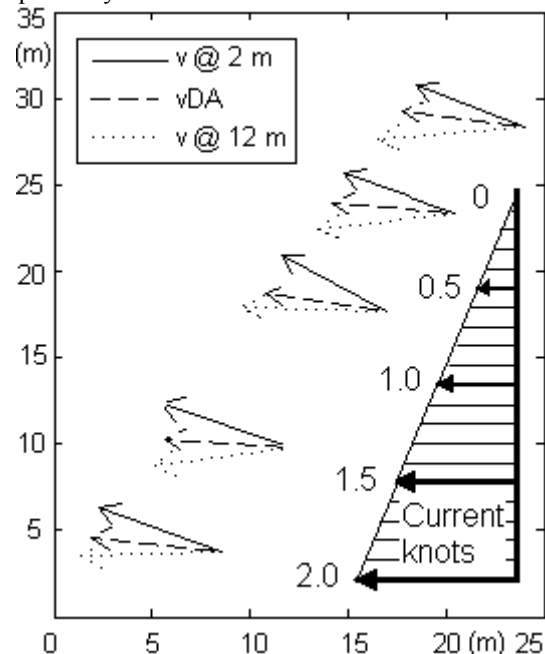


Figure 2 Area of interest showing velocities at different depths from transect A1 (Ref: Figure 3).

3 Discussion

Evidence of secondary flow is identified when the surface, depth average and bottom velocities are plotted in an area of interest. One would expect that the bottom velocity would be rotated inwards, and the top velocity would be rotated outwards in relation to the depth average velocity (Figure 2).

The main area of interest is in front of the Fergusson wharf, and downstream towards the Jellicoe wharf (Figure 3). This area displayed strong evidence of curvature induced secondary flow at peak flood tide, i.e., when the stream-wise flow is the strongest. The size of this area is approximately 250 m in width and extends approximately 500 m beyond the tip of the

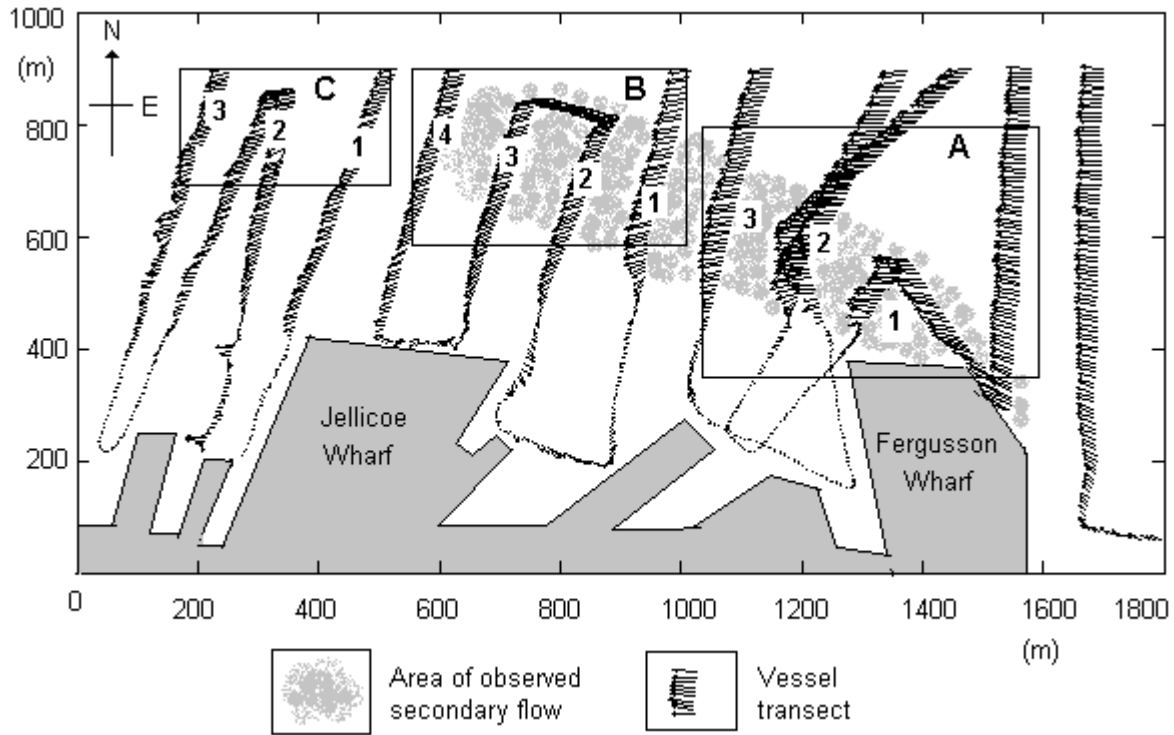


Figure 3 Map showing the area of observed secondary flow. The secondary flow is: Fully developed (area A), decaying (area B), and decayed (area C). The numbers indicate the individual transects used for Figure 8.

Fergusson wharf towards the front of the Jellicoe wharf (Transects A1 – B1, Figure 3). This is an area where the stream-wise flow is curved. There was slight, but inconclusive evidence of curvature induced secondary flow in the vicinity of the Wynyard wharf on the ebb tide.

The average cross-stream velocity normalised to the depth average for 99 raw profiles from *area A* are plotted against the normalised ADCP depth (Figure 4). The observed mean cross-stream velocity profile has the main features of the profiles from the model (Kalkwijk and Booij, 1986). These features are a linear slope over the mid water column and a near zero crossing at $z/h = -0.5$.

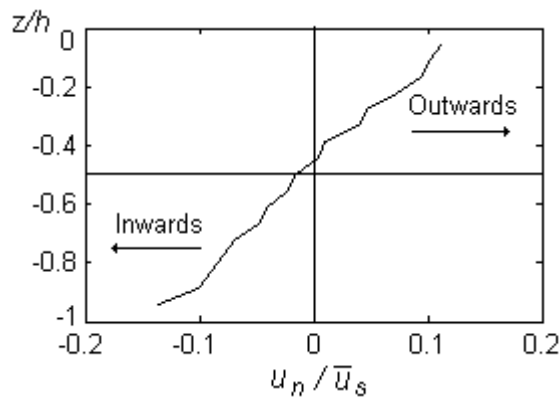


Figure 4 Average cross-stream velocity profile for area A (Ref: Figure 3).

The average stream-wise velocity is normalised by the depth average is plotted against the normalised ADCP depth (Figure 5). The observed mean stream-wise

velocity profile shows a 30 % reduction in velocity over the range of ADCP measurements due to bottom friction. The average stream-wise velocity profile also indicates a slight reduction in velocity towards the surface, which could be an indication of estuarine baroclinic flow as a result of fresh water draining into the Waitemata Harbour. Towards the bottom, the slope shows a more logarithmic shape consistent with a profile due bottom friction.

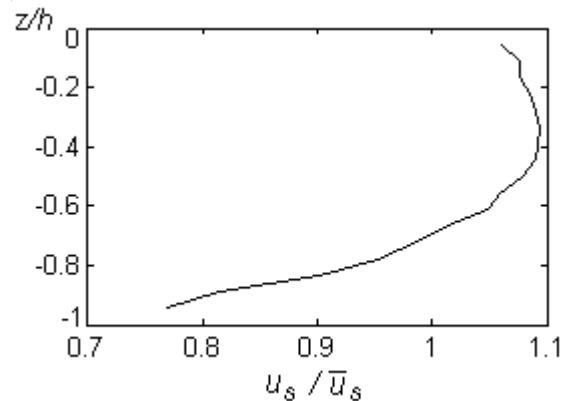


Figure 5 Average stream-wise velocity profile for area A (Ref: Figure 3).

To further investigate the reduction of velocity towards the surface the magnitude of the average velocity for all of circuits 2 and 3 are plotted against the normalised ADCP depth for both the flood and ebb tide (Figure 6). On the flood tide there is a slight reduction of velocity towards the surface, indicating that the incoming sea water may be retarded by the surface fresh water consistent with baroclinic flow. On the ebb tide the velocity increases towards the surface indicating the out going seawater is being enhanced by

the surface fresh water and the slope at peak ebb is linear as opposed to logarithmic near the surface. At the turn of the tide the surface water velocity lags the bottom water velocity with weak surface flow in the ebb direction and flow in the flood direction at depth. (Figure 7).

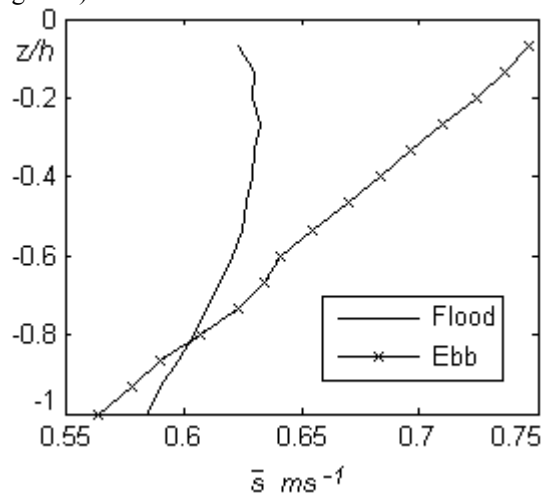


Figure 6 Average velocity magnitude for flood and ebb tide for all of circuit 2&3 (Ref: Figure 1).

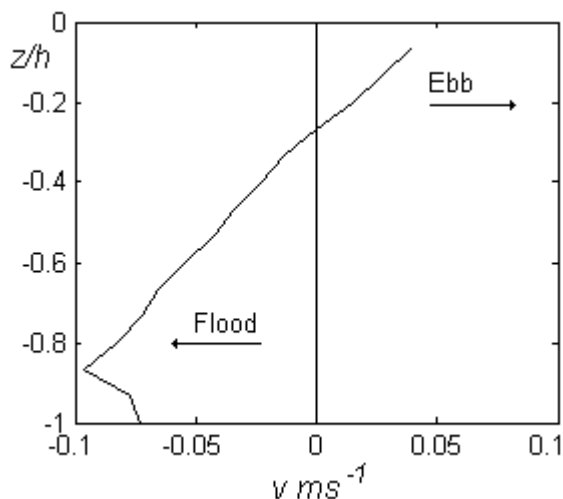


Figure 7 Average raw velocity at the turn of the tide for circuits 2 & 3 (Ref: Figure 1).

An analytical model has been developed for the gradual adaptation of secondary flow to changes in curvature (Kalkwijk and Booij, 1986). There is not enough upstream data to observe the development of secondary flow, there is however enough downstream data to observe the decay of secondary flow and roughly estimate the relaxation length. The relaxation length is the length after which secondary flow has reduced to \exp^{-1} or 37 % of it's original value, due to the disappearance of the driving force. The three areas A, B, & C shown in figure 3 correspond to areas of secondary flow that is developed, decaying, and decayed respectively. The un-normalised secondary flow is plotted against the normalised ADCP depth for individual transects within these three areas (Figure 8).

From the plot showing the decaying flow, transect B4, is roughly \exp^{-1} in value of transect B1. This corresponds to a distance of 350 m. This rough estimate has an uncertainty of ± 100 m, being the resolution between vessel transects in this area. This relaxation length is in the range predicted by the analytical model (Kalkwijk and Booij, 1986).

4 Conclusions

The normalised average cross-stream velocity profile shown in Figure 4 is linear in the mid-water column and has the mid-depth zero crossing as predicted by the model (Kalkwijk and Booij, 1986). The observed secondary flow is up to 9.0 cms^{-1} , or 10% of the peak stream-wise velocities. The stream-wise velocity profiles shown in Figures 5, 6 & 7, indicate a weak baroclinic flow in the stream-wise direction of approximately 10 cms^{-1} superimposed on the stronger tidal flow. This retards the surface velocities on the flood tide and increases them on the ebb tide.

The relaxation length of 350 m, or 20 water depths shows the scale of how the secondary flow adapts to changes in the driving force. The secondary flow is evident in the area where the stream-wise flow is curved and persists at full strength for 500 m past the tip of Fergusson wharf. The associated near bottom cross-stream flow has the potential to move sediment out of the channel towards the berthing area behind the wharf. In this area the stream-wise velocities are weak, which may lead to the accretion of sediment.

Acknowledgments

Ports of Auckland for the use of the data; Port hydrographic surveyors, Greg Cox and David Bate, who conducted the ADCP surveys.

References

- Bathurst, J., and R.D. Hay, Direct measurements of secondary currents in river bends, *Nature*, 269, 504-506, 1977.
- Garrett, C.J., and R. Loucks, Upwelling along the Yarmouth shore of Nova Scotia, *J. Fish. Res. Board. Can.*, 33, 116-117, 1976.
- Geyer, W. R., Three dimensional tidal flow around headlands, *J. Geophys. Res.*, 98, 995-966, 1993.
- Kalkwijk, J. and R. Booij, Adaptation of secondary flow in nearly-horizontal flow, *J. Hydraulic research*, 24, 19-37, 1986.
- Pingree, R., The formation of the Shambles and other banks by the tidal stirring of the seas, *J. Marine Biology Assoc.*, 58, 269-289, 1978.
- Vennell, R., and C.P. Old, High resolution observations of the intensity of secondary circulation along a curved tidal channel, *Submitted J. Geophys. Res.*, 2006.

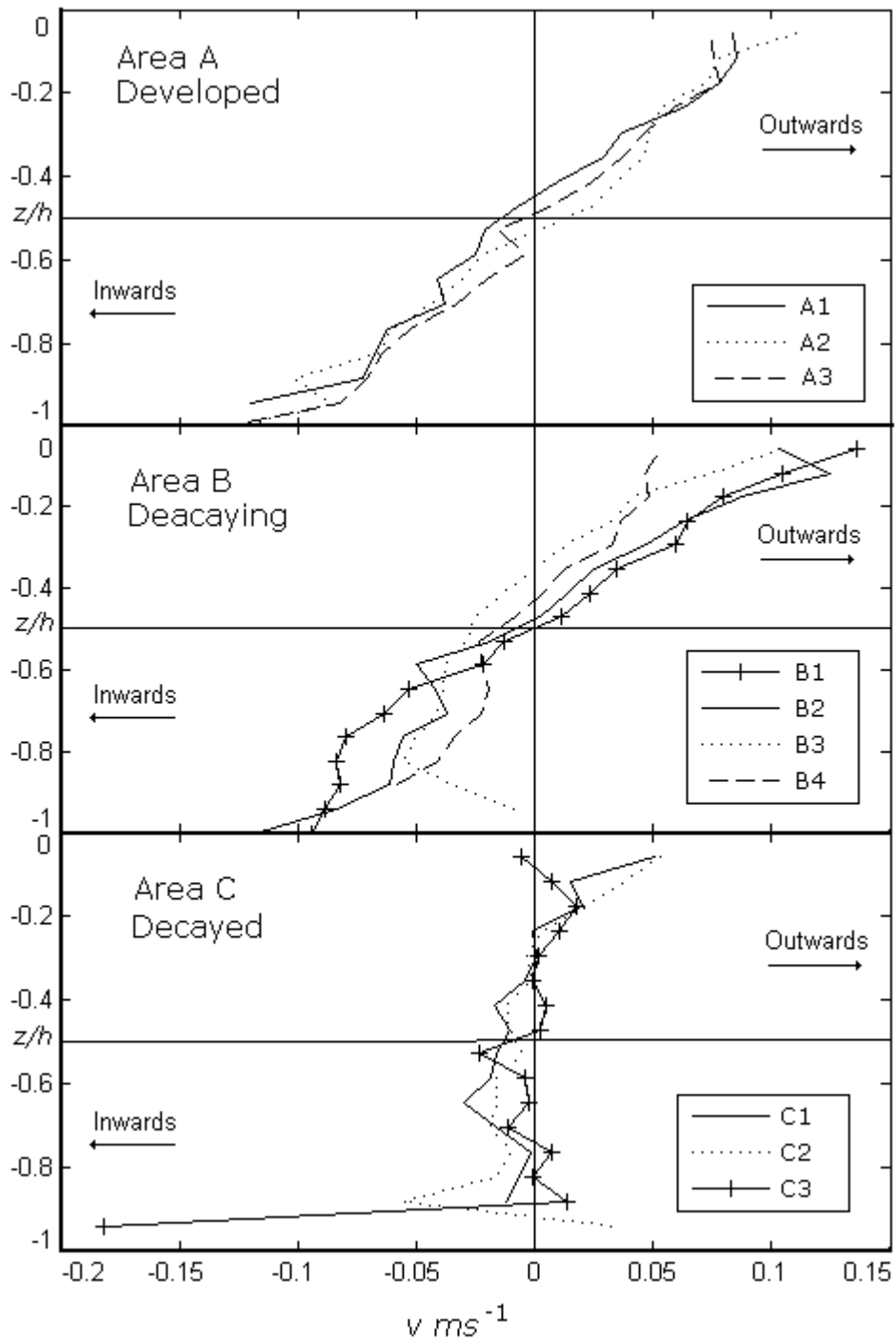


Figure 8 Average cross-stream velocities from individual transects (A1 - C3) showing the decay of secondary flow (Ref: Figure 3).